Photon migration in disordered media

S. Havlin, R. Nossal, B. Trus, and G. H. Weiss
National Institutes of Health, Bethesda, Maryland 20892
(Received 21 August 1991)

Numerical and analytical methods are used to study a model for the multiple scattering of photons in the presence of randomly reflecting inclusions. The photons are injected into a semi-infinite medium near its surface, and are absorbed by the surface or within the medium. In the medium the photons can diffuse only through voids between the reflecting inclusions, where the void structure has been modeled as a fractal object. Our analytical approach is based on an analogy between the kinetics of a continuous-time random-walk model and the movement of random walkers on fractals. For the case of nonabsorbing media, we find the survival of photons within the medium after n steps to be $S(n) \propto n^{-1+1/d_w}$ and the intensity profile at a distance ρ from the injection point to be $\Gamma(\rho) \propto \rho^{-d_w}$, where d_w is the diffusion exponent for fractals. For the case of absorbing media, $\Gamma(\rho)$ scales as $\mu^{\theta}\rho^{-\lambda}\exp(-\gamma\mu^{1/d_w}\rho)$, where μ is the absorption coefficient of the fractal medium, θ and λ are exponents related to the fractal dimensions, and γ is a constant. We also calculate the mean time and the average maximal depth of photons that emerge at a distance ρ.

PACS number(s): 42.25.Fx, 42.25.Bs, 87.71.Rh

I. INTRODUCTION

In recent years much effort has been devoted to developing remote-sensing techniques that use light to penetrate heterogeneous or locally disordered media. Examples are optically based medical diagnostic procedures that measure blood flow or hemoglobin oxygenation [1–7], and light detection and ranging (LIDAR) of the atmosphere [8,9] and ocean [10,11]. Related techniques, which do not involve light, are pressure-transient analysis of reservoirs [12,13] and seismographic procedures which depend on the propagation of sound waves [14]. Each of the above-mentioned processes involves multiple scattering of probe radiations which enter a randomly structured medium and then are subsequently detected when they are reemitted. Somewhat different technological schemes which depend on the interaction of radiation with multiple-scattering centers in inhomogeous media include the capture of light within metal-insulator composites [15,16] (used in solar-energy conversion devices) and neutron irradiation of radioactive wastes [17]. The random structure of the materials which are being probed affects the spatial and temporal distributions of the penetrating radiations. Because a high degree of multiple scattering occurs, a useful model of radiative transfer is that of the migration of localized packets of energy, which in the case of visible light can be described as individual photons [14,18].

In the present paper we investigate a model of photon penetration and migration in a disordered medium. The geometrical arrangement, which pertains to several remote-sensing technologies, considers photons to be inserted at one point of an interface and then detected at another point of that interface after having migrated through the underlying medium (Fig. 1). Specifically, we examine the properties of photon diffusion in a medium containing randomly distributed reflecting inclusions of varying sizes. These inclusions are assumed to fill so much space that they form an almost impenetrable barrier to photon transit between the surface optodes. The presence of such inclusions rules out the simplest approach to the analysis of such problems, generally based on classical transport or diffusion theory. Therefore, to allow investigation of more general random media, we have modified and used analytic techniques for photon migration that we previously developed to study laser Doppler flowmetry and time-resolved absorption spectroscopy in biological tissues [19–22]. Our present model

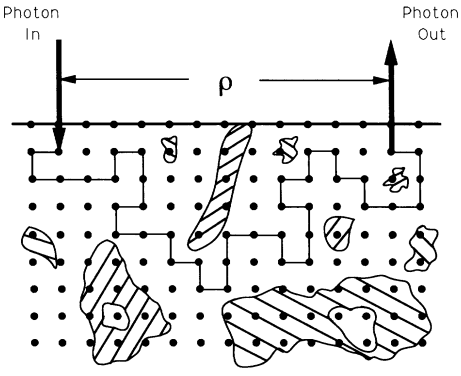

FIG. 1. Schematic representation of the model. Photons are inserted at a point on the surface of a semi-infinite scattering medium and emerge at a point ρ units of distance from the point of insertion. Distances between lattice points are related to the inverse of the bulk scattering cross section (see text). Shown is a hypothetical path of a photon as it moves on accessible lattice points (the "voids"). Shaded regions represent embedded reflectors.

considers photon transport within the medium in terms of a random walk on a fractal structure.

The analysis represents an initial effort to examine qualitative features expected in this class of models that might differ from those predicted by a diffusion theory. Inclusions within the medium are modeled in terms of a distribution of reflecting points on a lattice. Photons cannot move onto the reflecting sites, but they execute a random walk on the other lattice points (the "voids"), which therefore constitute a fractal object. A particularly useful case for simulations is a model based on a random walk on a square or cubic lattice. In this case, the probability that a given site is a reflector is equal to c, so that the concentration of sites on which the particles move is $p=1-c$. The motion of the photons on the void sites is equivalent to transport on a percolation system. When p is less than a critical concentration p_c, only finite clusters of voids exist and the motion of the photons is regionally restricted. We are interested in values $p>p_c$, where a spanning cluster of connected void sites exists, allowing photons that are launched on a such a cluster to move over long distances. This spanning cluster is characterized by a correlation length ξ such that, for distances smaller than ξ, the system can be regarded as a fractal medium. As p approaches p_c, the correlation length diverges ($\xi\rightarrow\infty$), and the system is fractal on all length scales. The critical concentrations for simple cubic lattices in two and three dimensions are $p_c=0.593$ ($D=2$) and $p_c=0.311$ ($D=3$) [23].

We use both numerical and analytical techniques in this study. The analytical approach is based on an analogy between movement on fractals and the evolution of probability densities in a continuous-time random-walk model. Results derived from the theory are, in all cases, shown to be compatible with numerical data.

The function of principal interest is the joint probability, $\Gamma(\rho,n)$, that a random walker will emerge from the surface of a semi-infinite medium at a distance ρ from the insertion point at step n (see Fig. 1). Throughout this paper we often refer to the migration of "photons" because of our interest in the multiple scattering of light, in which case $\Gamma(\rho,n)$ represents the intensity profile of diffusely reemitted light. In terms of a model of light propagation, we can identify ρ as $\rho=\Sigma_s d$, where d is the actual geometric distance on the surface, and Σ_s^{-1} is the distance between points on an equivalent isotropic scattering lattice [19]. The number of steps, n, can be related to real time as $n=\Sigma_s c_T t$, where c_T is the speed of light in the medium. The interfacial surface here is considered to be totally absorbing, so every photon that reaches the surface leaves without reflection. It has been shown, analytically, that when the medium is homogeneous and the interface is only partially reflecting, the result for $\Gamma(\rho,n)$ will be virtually unchanged unless the reflection is nearly total [24]. We assume this to be true as well in the present case. In homogeneous biological tissues, where photon-diffusion models seem to yield good representations of data [25], scattering primarily is caused by cell boundaries and interior organelles. Familiar examples of large biological entities that contain extended internal nonuniformities are bone and lung.

Initially we neglect internal absorption. In this case we find that $\Gamma(\rho,n)$ has a form whose ρ dependence differs for short and long times [Eq. (14)]. In both time regimes the concentration profile is non-Gaussian, in contrast to the functional form found for a uniform homogeneous medium [19,22,25]. The effect of the fractal nature of the inclusions is to concentrate the reemitted photons near the point of insertion [Eq. (15)]. Derivations of these and related results are given in Sec. II. Effects of internal absorption are considered in Sec. III. In addition to profiles of diffuse surface emission, we calculate the expected length of path $\langle n|\rho\rangle$ for photons that are trapped on the surface at a distance ρ from the entrance point. We also compute the average depth of photons that emerge on the surface at a distance ρ from the entrance point, $\langle z|\rho\rangle$. Finally, in Sec. IV, we consider the case where a diffusionlike theory is applicable, exemplified by percolation for $p>p_c$ and $\rho>\xi$, but where the diffusion coefficient depends on the density and nature of the inclusions.

II. PHOTON MIGRATION, NEGLECTING INTERNAL ABSORPTION

We model the medium as a semi-infinite three-dimensional system, and the interface as a planar absorbing surface (see Fig. 1). The material properties of the medium are assumed to be isotropic, and the coordinate system is chosen to be $\{x,y,z\}$, with x and y parallel to the interface, ranging from $-\infty$ to $+\infty$. The surface is specified by $z=0$, and positive values of z refer to points inside the medium. Because of the isotropy, the coordinates x and y will not appear separately, but only in the combination $\rho=(x^2+y^2)^{1/2}$. The point at which radiation is injected into the medium is designated as (0,0,1). The medium contains reflecting inclusions, distributed in such a way that photons move in a fractal space or in a percolation system.

To see how the fractal properties of the medium might influence the diffusion of radiation, we here neglect internal absorption. In this case, in the absence of an absorbing surface, the probability for the displacement of a random walker on a fractal, $P(r,n)$, has been determined by studies based on exact enumeration and scaling theories [26,27]. The probability of migrating a distance r as a result of an n time-step walk can be written in scaled form as [26,28]

$$P(r,n)=\frac{1}{n^{d_f/d_w}}g(u)\ , \tag{1}$$

where d_f represents the fractal dimension of the medium through which the random walker moves and d_w is the diffusion exponent defined by the mean-square displacement $\langle r^2\rangle=n^{2/d_w}$. The dimensionless spatial variable u is defined as $u=r/\langle r^2\rangle^{1/2}$, and $g(u)$ is given as

$$g(u)\propto\exp(-\alpha u^{d_w})\ ,\quad u\ll 1 \tag{2a}$$

or

$$g(u) \propto \exp(-\beta u^{\delta}) , \quad u \gg 1 \tag{2b}$$

where $\delta = d_w/(d_w - 1)$ and α and β are constants that relate to the detailed structure of the lattice and the random walk. There is extensive evidence, based on simulations [29], for the form shown in Eq. (2b) ($u \gg 1$), but much less for the complementary regime ($u \ll 1$) which is of principal importance in our study. Equation (2a) is substantiated, here, by exact enumeration of a random walk on a two-dimensional Sierpinski gasket of nine generations. (The exact enumeration method is explained in detail in Ref. [26].) Results are shown in Fig. 2, where $P(r,n)$, as given by Eq. (1), is demonstrated for both of the asymptotic regimes of u. In general, the expression given in Eq. (1) relates to an average over all possible realizations of the random walk.

To derive an expression characterizing photon migration in the presence of an absorbing surface, we relate our problem to a model of an anomalous random walk on a lattice which has been solved earlier [30]. This model, for which an exact analytical solution has been obtained, is a continuous-time random walk (CTRW) on a uniform lattice [31] where, at each site, the random walker remains for a variable time τ chosen according to the probability density $\psi(\tau)$. If we assume that, for large τ, $\psi(\tau) \propto \tau^{-(\alpha+1)}$, with $0 \leq \alpha \leq 1$, then one obtains anomalous transport, i.e., $\langle r^2 \rangle \propto t^{2/d_w}$, with $d_w = 2/\alpha$. A

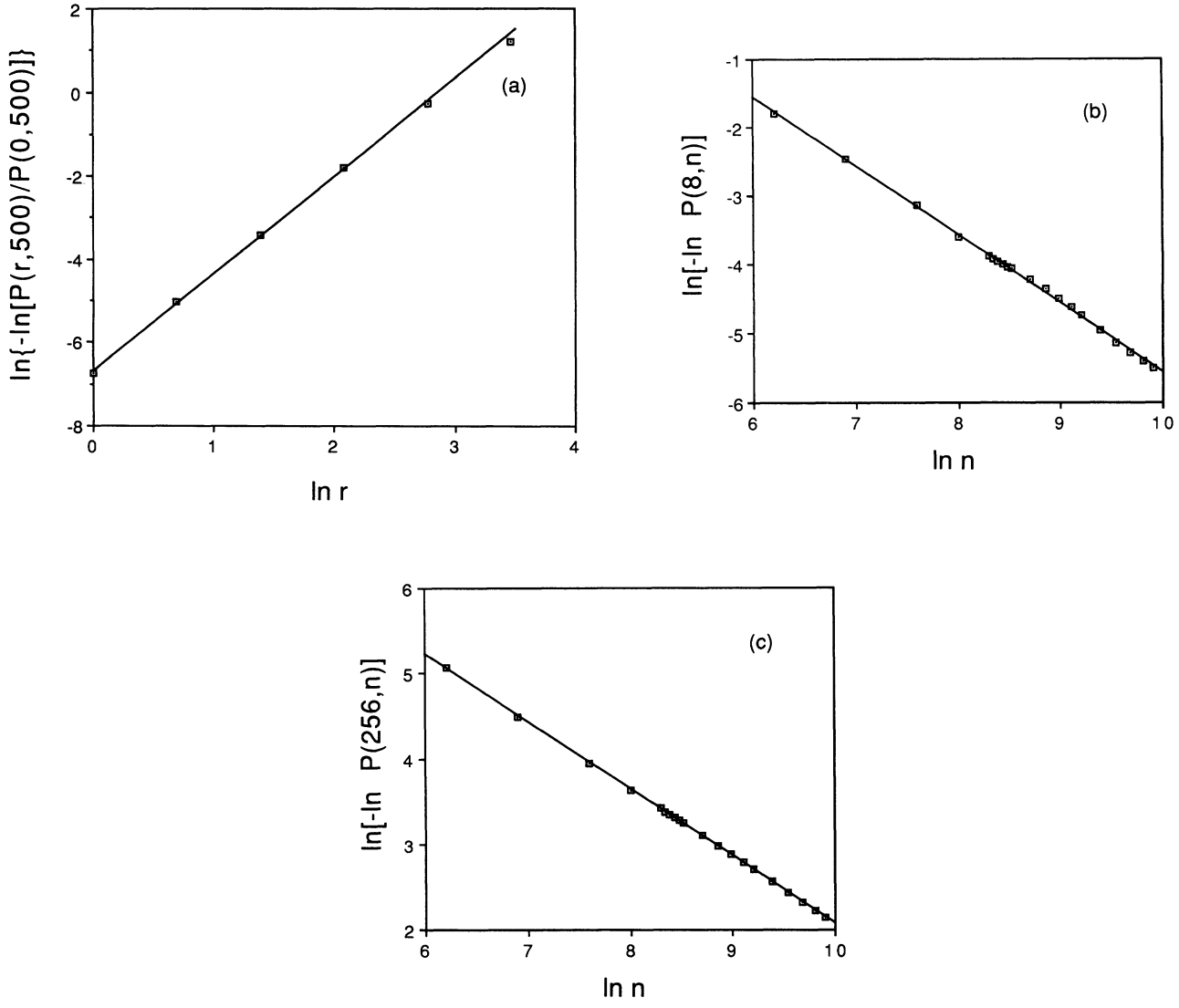

FIG. 2. Numerical results for $P(r,n)$ on a Sierpinski gasket of nine generations using the exact enumeration method: (a) Plot of $\ln\{-\ln[P(r,n)/P(0,n)]\}$ vs $\ln r$ for $n = 500$ in the regime $u \ll 1$. The slope is 2.31, in agreement with $d_w = \ln 5/\ln 2 = 2.32$, as indicated in the r exponent in Eq. (2a). (b) Plot of $\ln[-\ln P(r,n)]$ vs $\ln n$ for $r = 8$. The slope is -1.0, in agreement with the time dependence in Eq. (2a) for $u \ll 1$. (c) Plot of $\ln[-\ln P(r,n)]$ vs $\ln n$ for $r = 256$ in the regime $u \gg 1$. The slope is 0.78, in agreement with $\delta/d_w = 1/(d_w - 1) = 0.76$ from Eq. (2b).

correspondence between the CTRW and a random walk on a fractal can be established, in that the mean-square displacement $\langle r^2 \rangle$ for both processes has the same mathematical form [32] and a value of α can always be chosen to yield the value of d_w associated with a specific fractal. $P(r,n)$ (in the regime $u \gg 1$) is also known to have a similar structure in both theories, and the CTRW has been applied successfully to describe transport in amorphous solids [33,34] and transport on fractals [26,35].

One can also show by the method of images that $p_{\mathrm{CTRW}}(\rho,z,n)$, which is defined as the probability density (in the continuum limit) for the position, in the semi-infinite medium $z<0$, of the random walker at step n in the CTRW model in the presence of absorbing surface at $z=0$, is given as [30]

$$p_{\mathrm{CTRW}}(\rho,z,n) \propto n^{-d_f/d_w}\left[g\left[\frac{(\rho^2+(z-z_0)^2)^{1/2}}{n^{1/d_w}}\right]-g\left[\frac{(\rho^2+(z+z_0)^2)^{1/2}}{n^{1/d_w}}\right]\right] . \quad (3)$$

Here, z_0 is the depth at which the photons are injected. To calculate the probability density $p(\rho,z,n)$ for the position of the random walker on a fractal in the presence of an absorbing surface at $z=0$, we have to take into account the differences between the CTRW and the fractal models. Anomalous diffusion in this CTRW model occurs because the walker can stay at single sites of the system for long times. On the fractal, though, movement occurs at each time step, but the diffusion process is anomalous because the motion of the walker is affected by the self-similar nature of the matrix of the voids, which are connected by narrow pathways ("bottlenecks"). Due to these differences, the probability that a walker remains in the matrix differs in the two cases. We *assume* that $p(\rho,z,n)$ and $p_{\mathrm{CTRW}}(\rho,z,n)$ are related as

$$p(\rho,z,n) \propto A(\rho) p_{\mathrm{CTRW}}(\rho,z,n) , \quad \rho \leq n^{1/d_w} \quad (4)$$

and will show, later, that analytical expressions which follow are in agreement with numerical simulations.

In Eq. (4), $A(\rho)$ represents the ratio of the transition rates of the two processes, i.e., $A(\rho) \propto 1/\tau_{\mathrm{CTRW}}$, where τ_{CTRW} is the mean time that a random walker stays at a single site in the CTRW model. In order to estimate τ_{CTRW}, which can be interpreted as the average time per site transition, we note that the distance traveled on the lattice in the CTRW model can be expressed in terms of the number of site transitions, N, as $\langle \rho^2 \rangle \propto N$, whereas the distance scales with the number of time steps as $\langle \rho^2 \rangle^{d_w/2} \propto n$. Consequently, $\tau_{\mathrm{CTRW}} \propto n/N \propto \rho^{d_w-2}$, which leads to

$$p(\rho,z,n) \propto \rho^{2-d_w} p_{\mathrm{CTRW}}(\rho,z,n) . \quad (5)$$

The intuitive arguments which lead to Eq. (5) are substantiated by numerical simulations that are discussed later.

Let us next calculate the asymptotic survival probability $S(n)$ for a single photon. This quantity is the probability that the photon is still within the material at the nth step. The survival probability is calculated in terms of $p(\rho,z,n)$ in terms of a double integral

$$S(n) \propto \int_0^\infty \int_0^\infty p(\rho,z,n) \rho^{d_f-2} d\rho\, dz , \quad (6)$$

in which the term ρ^{d_f-2} accounts for the geometrical structure of the fractal and in which $p(\rho,z,n)$ is found by combining Eqs. (3) and (5). We first evaluate the integral over z, finding

$$\int_0^\infty p(\rho,z,n)\,dz \propto n^{-d_f/d_w} \int_{-z_0}^{z_0} g\left[\frac{(\rho^2+v^2)^{1/2}}{n^{1/d_w}}\right] dv , \quad (7)$$

where the function $g(u)$ is defined in Eq. (2). We next take advantage of the fact that $\rho^2 \gg z_0^2$ and that $g(u)$ is a smoothly varying function, which implies that the last integral can be approximated by

$$\int_{-z_0}^{z_0} g\left[\frac{(\rho^2+v^2)^{1/2}}{n^{1/d_w}}\right] dv \propto 2z_0 g\left[\frac{\rho}{n^{1/d_w}}\right] . \quad (8)$$

Thus, we find that the asymptotic time dependence of the survival probability for a photon on the fractal is determined from the integral

$$S(n) \propto 2z_0 n^{-d_f/d_w} \int_0^\infty \rho^{d_f-d_w} g(\rho/n^{1/d_w}) d\rho \propto n^{-1+1/d_w} , \quad (9)$$

in the limit of large n. Note that to derive Eq. (9), only the scaling form of $p(\rho,z,n)$ is needed, and not its specific functional form. Figure 3 shows results of numerical simulations of the survival probability based on the exact enumeration method, as a function of n on a log-log plot for three fractals: percolation (two and three dimensions) and the Sierpinski gasket. The results agree with the exponent calculated in Eq. (9), which also lends support to the reasoning leading to Eq. (5).

We can contrast the expressions given by Eq. (9) with the comparable result for the CTRW model in the presence of a trapping surface [30]:

$$S_{\mathrm{CTRW}}(n) \propto n^{-1/d_w} . \quad (10)$$

A glance at these equations makes it clear that the two survival probabilities, as indicated in Eqs. (9) and (10), differ considerably in their dependence on d_w. In the case of fractals, Eq. (9) indicates that when d_w increases, the survival probability decreases. In contrast, the survival probability in the CTRW model, Eq. (10), increases as d_w increases. To understand this difference, note that in the problem presently considered the random walker moves away from its position at every step, which is not the case for the comparable CTRW. The variable $\langle r^2 \rangle \propto n^{2/d_w}$

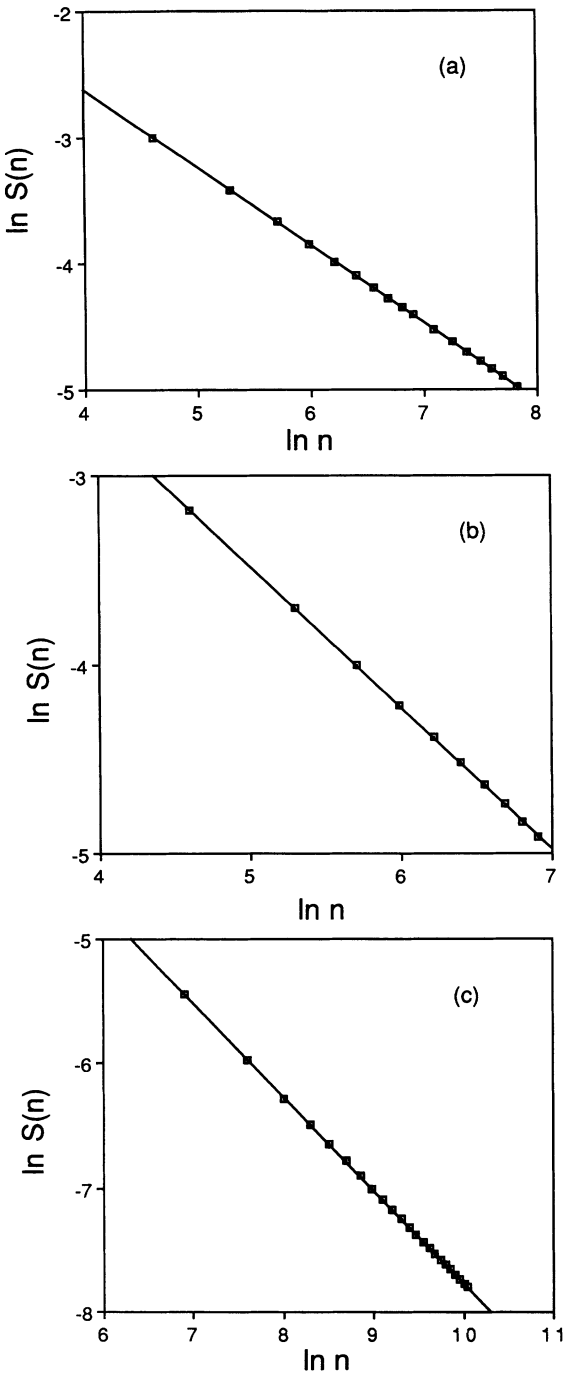

FIG. 3. Plot of $\ln S(n)$ vs $\ln n$ for three fractals obtained from numerical simulations. The percolation clusters were generated at criticality using the method of Leath [Phys. Rev. B **14**, 5046 (1976)]. (a) Percolation clusters at criticality in $d=2$; the slope is -0.62, in agreement with $-1+1/d_w=-0.64$ from Eq. (9). (b) Percolation clusters at criticality in $d=3$; the slope is -0.74, compared with $-1+1/d_w=-0.73$. (c) Sierpinski gasket (SG) in $d=2$; the slope is -0.75. [Note that for the SG, the integrand in Eq. (9) should be multiplied by ρ^{d_f-1}/ρ. Equation (9) was derived by assuming that the dimensionality of the absorbing surface is d_f-1 (such as in the case of percolation). However, in the SG the absorbing surface is a one-dimensional edge. This modification leads to $S(n)\propto n^{-1-1/d_w+d_f/d_w}$, whose exponent is 0.748, in agreement with the slope of the figure.]

indicates the displacement away from any given point at time n. In the case of the fractal, the displacement decreases because the photon is constantly "bumping into" the inclusions and the probability of returning to and being trapped at the surface increases [see Eq. (9)]. In the CTRW, in contrast, a slowdown in motion is accomplished by forcing the random walker to remain in the same location, which means that the rate at which it explores its neighborhood and reaches the surface is diminished [36].

It is easy to calculate the integrated surface flux, defined as the total number of photons absorbed by the surface per unit time. We immediately find, from Eq. (9),

$$\Gamma(n)=-\frac{dS(n)}{dn}\propto n^{-(2-1/d_w)} . \tag{11}$$

Another property of interest is the surface flux at a distance ρ from the entry point, $\Gamma(\rho,n)$. This quantity is the probability density that a photon is absorbed at the surface, at a distance ρ at step n. To calculate $\Gamma(\rho,n)$, we start with the following expression [30]:

$$\Gamma(\rho,n)\propto n^{2/d_w-1}p(\rho,1,n) , \tag{12}$$

which has been derived for the CTRW. Equation (12) relates the number of walkers absorbed by the surface at the nth time step to the probability density just below the surface (at $z=z_0=1$) at the $(n-1)$th step, $p(\rho,1,n-1)$. Due to the fractal nature of the accessible space, the probability of being absorbed depends also on the factor n^{2/d_w-1}. This factor is the fraction of time that a random walker, which lies just below the surface, is on a site which is a nearest neighbor to the surface (i.e., directly connected), so that on its next transition it can be absorbed. (In a Euclidean space, for which $d_w=2$, n^{2/d_w-1} is a constant whose value depends on the lattice [19].)

An expression for $p(\rho,1,n)$ can be obtained from Eqs. (3) and (5) for $\rho>z_0$, with different behaviors in the two regimes of time indicated in Eq. (2). Hence, we find

$$p(\rho,1,n)=\begin{cases} n^{-1-d_f/d_w}e^{-b\rho^{d_w}/n} , & \rho/n^{1/d_w}\ll 1 \\ n^{-1/(d_w-1)-d_f/d_w}\rho^{\delta-d_w}e^{-c(\rho/n^{1/d_w})^{\delta}} , & \end{cases} \tag{13a}$$

$$\rho/n^{1/d_w}\gg 1 , \tag{13b}$$

where b and c are constants and $\delta=d_w/(d_w-1)$. Thus, in accordance with Eq. (12), the quantity $\Gamma(\rho,n)$ is given as

$$\Gamma(\rho,n)\propto\begin{cases} n^{2/d_w-2-d_f/d_w}e^{-b\rho^{d_w}/n} , & \rho/n^{1/d_w}\ll 1 \\ n^{2/d_w-\delta/d_w-d_f/d_w-1}e^{-c(\rho/n^{1/d_w})^{\delta}} , & \end{cases} \tag{14a}$$

$$\rho/n^{1/d_w}\gg 1 . \tag{14b}$$

We note that the scaling behavior of the intensity profile on the surface, after integration over all time, can be derived from the scaling properties of Eqs. (1), (3), (4), and (14a) according to

$$\gamma(\rho)\equiv 2\pi\rho^{d_f-2}\Gamma(\rho)\propto\int_0^\infty \rho^{d_f-2}\Gamma(\rho,n)dn$$
$$\propto\int_0^\infty n^{2/d_w-2-d_f/d_w}\rho^{d_f-2}\times g(\rho/n^{1/d_w})dn\propto\rho^{-d_w}. \quad (15)$$

The spatially integrated flux of walkers trapped by the surface can be obtained, similarly, as

$$\Gamma(n)=\int_0^\infty \Gamma(\rho,n)\rho^{d_f-2}d\rho\propto n^{-(2-1/d_w)}. \quad (16)$$

Both results indicate the consistency of our arguments: Eq. (16) agrees with Eq. (11), and Eq. (15) agrees with the simulated numerical data shown in Fig. 4.

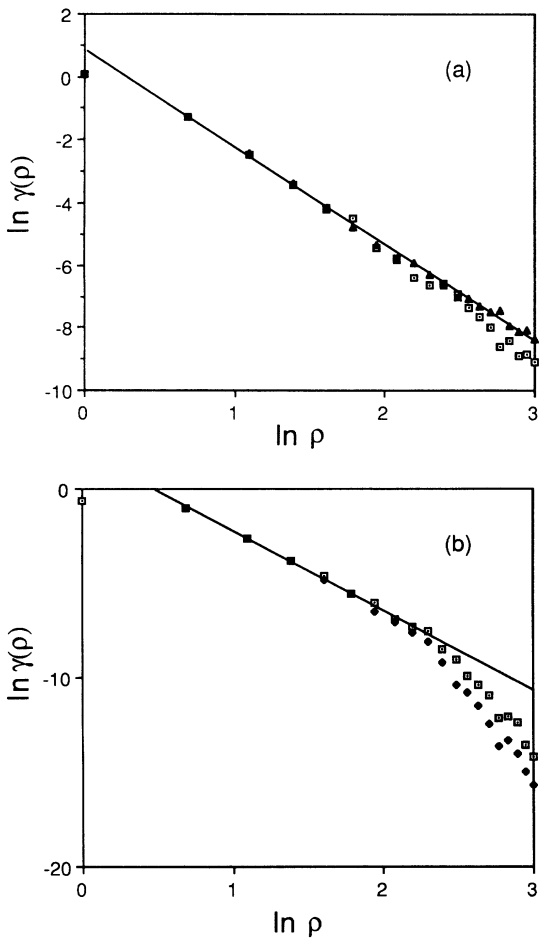

FIG. 4. Data from numerical simulations of random walks on percolation fractals. Plot of $\ln\gamma(\rho)$ vs ρ for (a) $d=2$ and (b) $d=3$ percolation at criticality. The slopes are 2.9 and 3.7, in agreement with Eq. (15). In each diagram, the two symbol types represent different times up to which $\gamma(\rho)$ has been calculated. The upper symbols represent longer times, with better convergence to a line having a slope of d_w, in accordance with Eq. (15). (For percolation, d_w is known to be 2.87 and 3.8, in two and three dimensions.)

III. PHOTON MIGRATION IN AN ABSORBING MEDIUM

The existence of internal absorption leads to significant changes in several physically interesting properties. We now modify the theory by assuming that, on each step, the random walker, when moving on the fractal lattice, has a finite probability of being absorbed. We designate that probability as $1-\exp(-\mu)$. Hence, if $\Gamma(\rho,n|\mu)$ is denoted as the intensity profile at the surface in this more general case, we can relate $\Gamma(\rho,n|\mu)$ to $\Gamma(\rho,n)$ [see Eq. (14)] by

$$\Gamma(\rho,n|\mu)=\Gamma(\rho,n)e^{-n\mu}. \quad (17)$$

To calculate the intensity profile $\Gamma(\rho)$ in the presence of absorption, we integrate Eq. (17) over all values of n. The presence of absorption tends to diminish the importance of photons that make long excursions. Consequently, only small values of the time are significant, which implies that the results of principal interest come from the regime $\rho/n^{1/d_w}\gg 1$. Therefore, we use the expression for $\Gamma(\rho,n)$ given in Eq. (14b) and evaluate the following expression:

$$\Gamma(\rho)\propto\int_0^\infty n^{2/d_w-\delta/d_w-d_f/d_w-1}e^{-c(\rho/n^{1/d_w})^\delta-\mu n}dn. \quad (18)$$

For large ρ, the dominant contribution to this integral comes from the neighborhood of that value of n that minimizes the absolute value of the exponent. Thus, the integral can be evaluated approximately by Laplace's method, which leads to the formula

$$\Gamma(\rho)\propto\mu^\theta\rho^{-\lambda}e^{-\gamma\mu^{1/d_w}\rho}, \quad (19)$$

where γ is a constant,

$$\theta=(d_f+\delta/2-2)/\delta d_w,$$

and $\lambda=(\theta+\frac{1}{2})\delta$. Data from numerical simulations of $d=2$ percolation at criticality, which are plotted in Fig. 5, tend to substantiate the prediction of this equation. Note that this result is a generalization of the expression given for a homogeneous medium [19],

$$\Gamma(\rho)\propto\mu^{1/2}\rho^{-2}\exp(-A\rho\sqrt{\mu}),$$

which is obtained from Eq. (19) by choosing $d_f=3$ and $d_w=2$. For a fractal, $\Gamma(\rho)$ can exhibit a very different dependence on ρ and μ: For three-dimensional percolation at criticality, for example, one has $d_f\simeq 2.5$ and $d_w\simeq 3.8$, which implies that $\lambda\simeq 1.0$, $\theta\simeq 0.23$, and

$$\Gamma(\rho)\propto\mu^{0.23}\rho^{-1.0}\exp(-\gamma\mu^{0.26}\rho).$$

Until now we have concentrated on calculating the surface intensity $\Gamma(\rho,n|\mu)$. Other parameters relating to the photon path often are of interest [19]. One example is the expected length of path for photons that are trapped on the surface at a distance ρ from the entrance point, $\langle n|\rho\rangle$. For a homogeneous medium, this quantity may be calculated directly in terms of $\Gamma(\rho,n|\mu)$ as

$$\langle n|\rho\rangle=\frac{\Sigma_n n\Gamma(\rho,n|\mu)}{\Sigma_n\Gamma(\rho,n|\mu)}\propto\frac{\int_0^\infty n\Gamma(\rho,n|\mu)dn}{\int_0^\infty\Gamma(\rho,n|\mu)dn}\ . \quad (20)$$

In the case of a fractal medium, though, it is convenient to calculate the expected path length in terms of the so-called "chemical length" l, which is the shortest path length between two accessible sites [26,37]. The chemical length is related to the geometric distance ρ by $\rho\propto l^{\tilde{\nu}}$, where, for the percolation cluster at criticality, $\tilde{\nu}\simeq 0.88$ ($D=2$) and $\tilde{\nu}\simeq 0.75$ ($D=3$) [38]. The analog of Eq. (14b) for the quantity $\Gamma(l,n|\mu)$ can be shown [26] to have the form

$$\Gamma(l,n|\mu)\propto n^{2/d_w^l-\delta_l/d_w^l-d_l/d_w^l-1}e^{-c(l/n^{1/d_w^l})^{\delta_l}-\mu n}\ , \quad (21)$$

where $d_l\equiv\tilde{\nu}d_f$, $d_w^l\equiv\tilde{\nu}d_w$, and $\delta_l\equiv d_w^l/(d_w^l-1)$. When we substitute this expression into Eq. (20) and evaluate the resulting integrals approximately by using Laplace's method, we find

$$\langle n|l\rangle\propto l/\mu^{1/\delta_l}\ , \quad (22a)$$

which, because $\rho\propto l^{\tilde{\nu}}$, is equivalent to

$$\langle n|\rho\rangle\propto\rho^{1/\tilde{\nu}}/\mu^{1/\delta_l}\ . \quad (22b)$$

Note that $\langle n|\rho\rangle$ no longer is proportional to ρ, as is the case for a homogeneous medium. Simulated data support the relation just given. For example, Fig. 6, which has been obtained from numerical simulation, is a plot, on a logarithmic scale, of $\langle n|\rho\rangle$ as a function of ρ for the two-dimensional percolation cluster. The estimated slope 1.15 is in good agreement with the predicted value $1/\tilde{\nu}\simeq 1.14$ (Ref. [38]). Equation (22a) is similar in form to an expression obtained for homogeneous media

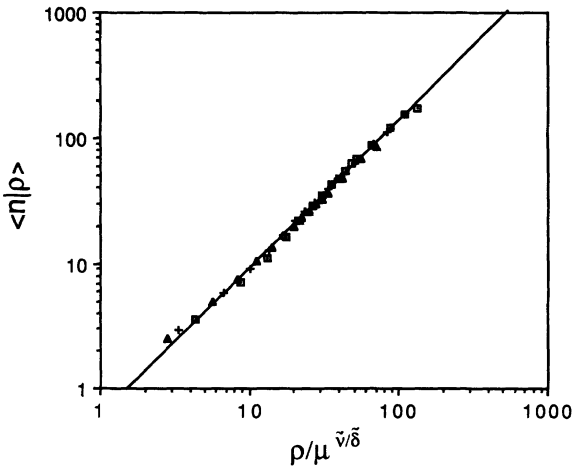

FIG. 6. Plot of $\langle n|\rho\rangle$ vs. $\rho/\mu^{\tilde{\nu}/\delta_l}$ on a log-log scale for $\mu=0.1$ (□), 0.15 (+), and 0.2 (△). The scaling and the slope of 1.15 agree with Eq. (22b).

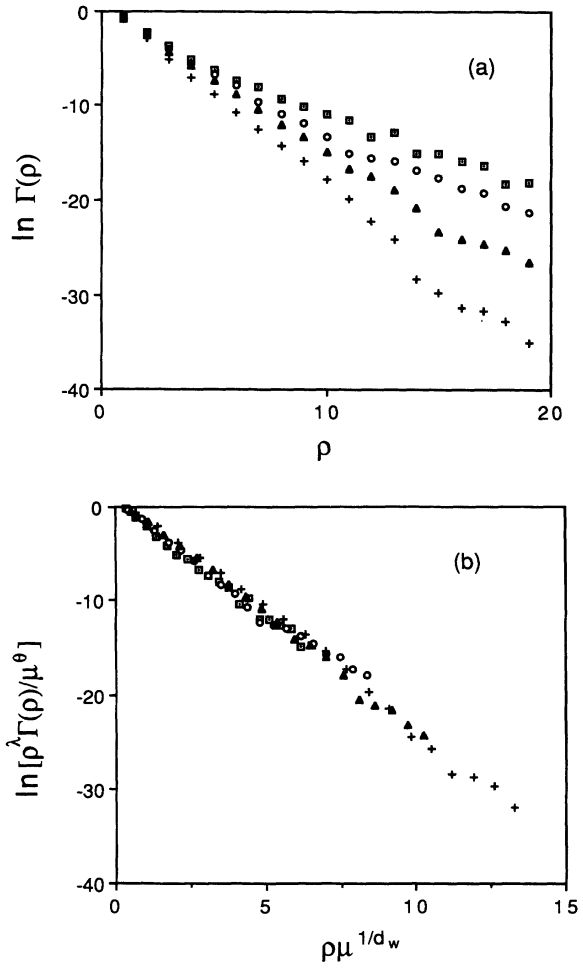

FIG. 5. (a) $\ln\Gamma(\rho)$ vs ρ for several values of μ, for $d=2$ percolation at criticality: $\mu=0.05$ (□), $\mu=0.1$ (○), $\mu=0.2$ (△), and $\mu=0.4$ (+). (b) Plot of $\ln[\rho^\lambda\Gamma(\rho)/\mu^\theta]$ as a function of $\rho\mu^{1/d_w}$. The scaling is in agreement with the prediction of Eq. (19).

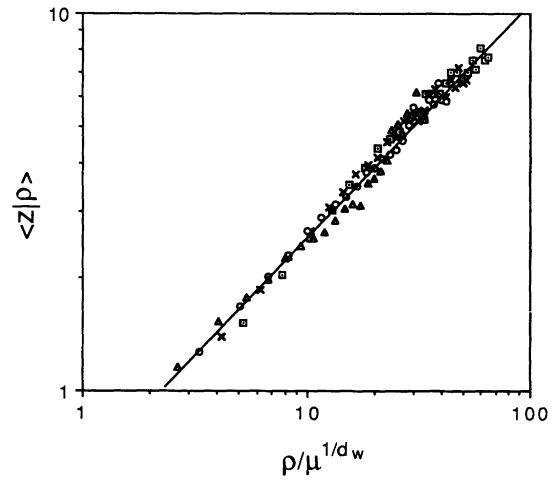

FIG. 7. Plot of $\langle z|\rho\rangle$ vs $\rho/\mu^{1/d_w}$ for $\mu=0.05$ (□), 0.1 (x), 0.2 (○), and 0.4 (△). The scaling and the slope of 0.6 support Eq. (23), where the predicted exponent is $1/2\tilde{\nu}=0.57$.

[19], viz., $\langle n|\rho\rangle \propto \rho/\mu^{1/2}$ (for large ρ), in that the dependence on distance is linear. On average, those photons which reach the surface travel along relatively short paths; photons having longer path lengths tend to be absorbed within the medium. In the homogeneous case, the metric of shortest distance is the Euclidean distance ρ, whereas on a fractal the shortest distances are the chemical lengths. Equation (22b) arises because the shortest paths on a fractal are not linear in ρ, but vary proportionally with $l \propto \rho^{1/\tilde{\nu}}$.

A second quantity of some interest is the average depth along the trajectory of photons that emerge on the surface at a distance ρ from the entrance point. This will be denoted by $\langle z|\rho\rangle$. Using essentially the same argument as in Ref. [39], one can show

$$\langle z|\rho\rangle \propto l^{1/2}/\mu^{1/2d_w^l} \propto \rho^{1/2\tilde{\nu}}/\mu^{1/2d_w^l} . \tag{23}$$

Figure 7, which contains a logarithmic plot of $\langle z|\rho\rangle$ as a function of ρ (obtained from numerical simulation), is in good agreement with this formula, and the scaling of different values of μ also is in agreement with this prediction.

IV. MIGRATION IN A PERCOLATION SYSTEM ABOVE CRITICALITY

When properties of the medium are strictly uniform, one can represent the migrating photon either in terms of a random walker or in terms of a diffusing particle. Both approaches give similar results [19,25]. We here make use of a modified diffusion theory.

Let $p(\mathbf{r},t|\mathbf{r}_0)$ be the probability density for the position of a photon at step n, given that it initially was at $\mathbf{r}_0$ [$=(0,0,z_0)$]. This function satisfies the diffusion equation [25]

$$\frac{1}{c_T}\frac{\partial p}{\partial t} = D_{op}\nabla^2 p - \Sigma_a p , \tag{24}$$

where the parameter Σ_a represents the cross section for internal absorption and, as before, c_T is the speed of light. The coefficient D_{op} is given as $D_{op}=(3\Sigma_s)^{-1}$ and has the units of length. The solution to Eq. (24), subject to the boundary condition

$$p(x,y,0;t|0,0,z_0)=0$$

together with the initial condition

$$p(\mathbf{r},0|\mathbf{r}_0)=\delta(\mathbf{r}-\mathbf{r}_0) ,$$

is

$$p(\mathbf{r},t|\mathbf{r}_0)=\frac{1}{8(\pi D_{op}c_T t)^{3/2}}\exp\left[-\frac{r^2}{4D_{op}c_T t}-\Sigma_a c_T t\right] \times\left[\exp\left[-\frac{(z-z_0)^2}{4D_{op}c_T t}\right]-\exp\left[-\frac{(z+z_0)^2}{4D_{op}c_T t}\right]\right] . \tag{25}$$

On identifying the reemitted radiation as the flux of photons through the surface, one finds the instantaneous surface intensity $\Gamma(\rho,t)$ to be given by

$$\Gamma(\rho,t)=D_{op}c_T\left.\frac{\partial p}{\partial z}\right|_{z=0} =\frac{z_0}{8(\pi D_{op}c_T)^{3/2}t^{5/2}} \times\exp\left[-\frac{\rho^2+z_0^2}{4D_{op}c_T t}-\Sigma_a c_T t\right] . \tag{26}$$

[Note that, in Eq. (26) and the following, ρ and z_0 are measured in terms of real spatial variables.]

The surface intensity $\Gamma(\rho)$ is found by integrating $\Gamma(\rho,t)$ over t,

$$\Gamma(\rho)=\int_0^\infty \Gamma(\rho,t)dt =\frac{z_0}{2\pi(D_{op}c_T)^{1/2}(\rho^2+z_0^2)}\left[1+\left[\frac{D_{op}}{\Sigma_a(\rho^2+z_0^2)}\right]^{1/2}\right] \times\exp\{-[\Sigma_a(\rho^2+z_0^2)/D_{op}]^{1/2}\} . \tag{27}$$

In the analysis which follows, we assume that $\rho^2 \gg z_0^2$ and $\rho(\Sigma_a/D_{op})^{1/2} \gg 1$, which means that $\Gamma(\rho)$ can be represented as [19]

$$\Gamma(\rho) \propto \rho^{-2}\exp(-\rho\sqrt{\Sigma_a/D_{op}}) \tag{28}$$

for large ρ. The only change in considering the same problem in d dimensions is that the prefactor ρ^{-2} in this equation is replaced by $\rho^{-(d+1)/2}$, but the form of the exponent remains unchanged (e.g., in two dimensions the prefactor is $\rho^{-3/2}$). We expect, when the concentration of sites on which the photons move (the voids) is greater than p_c, that the form of $\Gamma(\rho)$, for $\rho > \xi$, is like that shown in Eq. (28) (or its equivalent in d dimensions), but that the diffusion constant D_{op} would be replaced by a function of p. By modeling the diffusion by a random

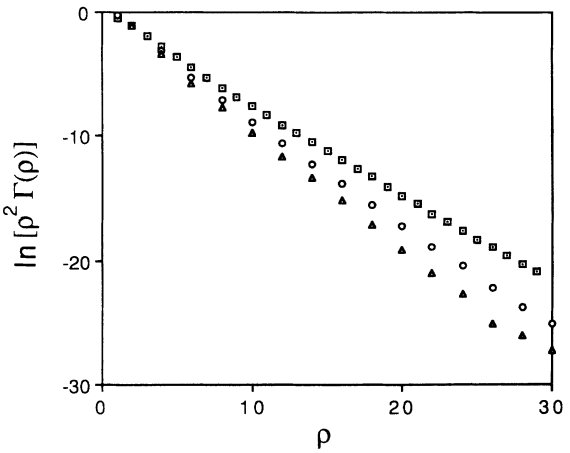

FIG. 8. (a) Plot of $\ln\rho^2\Gamma(\rho)$ as a function of ρ for several reflector concentrations $c \equiv 1-p$: $c=0.1$ (□), 0.3 (○), and 0.4 (△). The linear curves support Eq. (28).

walk, using the method of exact enumeration [26], we calculated $\Gamma(\rho)$ for several values of p. Results for $\ln\Gamma(\rho)$, plotted as a function of ρ, are shown in Fig. 8. The nearly straight lines support our conjecture.

We expect that when p approaches p_c, the motion of the walker will be severely restricted, implying $\lim p \to p_c D(p) = 0$. For values of p close to p_c, the following scaling argument yields

$$D_{op} c_T \propto \frac{\langle r^2 \rangle}{t} \propto \frac{\xi^2}{t} \propto \frac{\xi^2}{\xi^{d_w}} \propto (p - p_c)^{\nu(d_w - 2)} , \quad (29)$$

which indicates how the effective scattering cross section changes due to the inclusions [i.e., $\Sigma_s \propto (p - p_c)^{-\nu(d_w-2)}$]. The exponent $\nu(d_w - 2)$ appearing in this equation is, for the percolation model, equal to 1.16 in two dimensions and equal to 1.54 in three dimensions.

[1] M. Stern, Nature (London) **254**, 56 (1975).
[2] R. Bonner and R. Nossal, Appl. Opt. **20**, 2097 (1981).
[3] *Laser-Doppler Blood Flowmetry,* edited by A. P. Shepherd, Jr. and P. Å. Öberg (Kluwer Academic, Boston, 1990).
[4] K. K. Tremper and S. J. Barker, Anesthesiology **70**, 98 (1989).
[5] J. M. Schmitt, G. X. Zhou, E. C. Walker, and R. T. Wall, J. Opt. Soc. Am. A **14**, 2141 (1990).
[6] D. T. Delpy, M. Cope, P. van de Zee, S. Arridge, S. Wray, and J. Wyatt, Phys. Med. Biol. **33**, 1433 (1988).
[7] B. Chance, J. S. Leigh, H. Miyake, D. S. Smith, S. Nioka, R. Greenfeld, M. Finander, K. Kaufmann, W. Levy, M. Yound, P. Cohen, H. Yoshioka, and R. Boretsky, Proc. Nat. Acad. Sci. U.S.A. **85**, 4971 (1988).
[8] F. G. Fernald, Appl. Opt. **23**, 652 (1984).
[9] J. D. Klett, Appl. Opt. **24**, 1638 (1985).
[10] H. R. Gordon, R. C. Smith, and J. R. V. Zaneveld, Proc. Soc. Photo-Opt. Instrum. Eng. **489**, 2 (1984).
[11] M. A. Blizard, Proc. Soc. Photo-Opt. Instrum. Eng. **637**, 2 (1986).
[12] J. Chang and Y. C. Yortsos, SPE Form. Eval. (March, 1990), p. 31.
[13] R. A. Beier (unpublished).
[14] B. White, P. Sheng, M. Postel, and G. Papanicolaou, Phys. Rev. Lett. **63**, 2228 (1989).
[15] S. Berthier and J. Lafait, Thin Solid Films **125**, 171 (1985).
[16] S. Berthier, K. Driss-Khodja, and J. Lafait, J. Phys. (Paris) **48**, 601 (1987).
[17] P. Grand, Nature (London) **278**, 693 (1979).
[18] S. Feng and P. A. Lee, Science **251**, 633 (1991).
[19] R. Bonner, R. Nossal, S. Havlin, and G. H. Weiss, J. Opt. Soc. Am. A **4**, 423 (1987).
[20] R. Nossal, J. Kiefer, G. H. Weiss, R. Bonner, H. Taitelbaum, and S. Havlin, Appl. Opt. **27**, 3382 (1988).
[21] R. Bonner, R. Nossal, and G. H. Weiss, in *Photon Migration in Tissues,* edited by B. Chance (Plenum, New York, 1989), p. 11.
[22] R. Nossal, R. F. Bonner, and G. H. Weiss, Appl. Opt. **28**, 2238 (1989).
[23] D. Stauffer, *Introduction to Percolation Theory* (Taylor and Francis, London, 1985); *Fractals and Disordered Systems,* edited by A. Bunde and S. Havlin (Springer-Verlag, Berlin, 1991).
[24] D. Ben-Avraham, H. Taitelbaum, and G. H. Weiss, Lasers in the Life Sciences **4**, 29 (1991).
[25] M. Patterson, B. Chance, and B. C. Wilson, Appl. Opt. **28**, 2331 (1989).
[26] S. Havlin and D. Ben-Avraham, Adv. Phys. **36**, 695 (1987).
[27] A. Aharony and A. B. Harris, J. Stat. Phys. **54**, 1091 (1989).
[28] S. Alexander and R. Orbach, J. Phys. Lett. (Paris) **43**, L625 (1982).
[29] A. Bunde, S. Havlin, and E. H. Roman, Phys. Rev. A **42**, 6274 (1990).
[30] G. H. Weiss and S. Havlin, J. Stat. Phys. **63**, 1005 (1991).
[31] E. W. Montroll and G. H. Weiss, J. Math. Phys. **6**, 167 (1965).
[32] H. Weissman, G. H. Weiss, and S. Havlin, J. Stat. Phys. **57**, 301 (1989).
[33] H. Scher and M. Lax, Phys. Rev. **137**, 4491 (1973); **137**, 4502 (1973).
[34] H. Scher and E. W. Montroll, Phys. Rev. B **12**, 2455 (1975).
[35] G. H. Weiss and S. Havlin, Philos. Mag. B **56**, 941 (1987).
[36] The CTRW can be mapped onto a space of higher dimensionality which has comblike features, and where transitions occur at discrete time steps [26,35]. Thus, the CTRW is a process in which the anomaly arises when the number of accessible sites is increased, while the anomalous motion of photons on fractal objects is accompanied by a decrease in the volume of embedded sites.
[37] S. Havlin and R. Nossal, J. Phys. A **17**, L427 (1984).
[38] H. J. Herrmann and H. E. Stanley, J. Phys. A **21**, L1169 (1988).
[39] G. H. Weiss, R. Nossal, and R. F. Bonner, J. Mod. Opt. **36**, 349 (1989).